UBMISSION TO SPSC

NA64 Status Report 2023

The NA64 Collaboration[1]

ABSTRACT:
In this report, we summarise the 2016-2022 combined analysis on $A' \to$ invisible searches with 9.37×10^{11} electrons on target. With such statistics, NA64 started probing for the first time the well-motivated region of parameter space suggested by benchmark Light Dark Matter models, thus making further searches extremely exciting and important. In addition, the experiment has significantly extended its physics potential exploiting the use of positron and muon beams. This year, we present the first results obtained at H4 using 100 GeV positrons and at M2 using 160 GeV muons. Both techniques would allow to improve the LDM sensitivity at higher dark photon masses. Finally, we will also report on the two runs carried out in 2023 at H4 and M2 beam lines and conclude with an overview of our plans for the next year.

CERN-SPSC-2023-023 / SPSC-SR-332
31/08/2023

[1] http://na64.web.cern.ch/

Contents

1 Introduction

The quest for Dark Matter (DM) is one of the most pressing questions in particle physics. Scenarios suggesting the presence of a dark or hidden sector (DS) feebly interacting with the visible sector via a Dark Photon, are very well-motivated as they are simple and predictive. In particular, Light Dark Matter (LDM) models provide Weakly Interacting Massive particles (WIMP)-like candidates but in a broader and lower (sub-GeV) mass range, relating the cosmological observation with the Standard Matter (SM)-Dark Matter interaction. This turns out in a well-defined target region for accelerator-based and DM direct detection experiments. In this report, we present the latest LDM searches carried out with the 2016-2022 collected data at H4 beam line corresponding to 9.37×10^{11} electrons on target (EOT) [1]. The analysis demonstrates the robustness of our technique with a total background of 0.51 ± 0.13. No signal events compatible to $A' \rightarrow$ invisible decay have been found allowing us to set the most stringent upper limits in the kinetic missing ϵ and A' mass plane for masses below 350 MeV. We also demonstrate that the addition of the annihilation channel with the secondary positrons of the electromagnetic shower enhances our sensitivity in the high mass region. Moreover, our results constrain the values of scalar and Majorana DM with coupling $\alpha_D \leq 0.1$ and $m_{A'} > 3m_\chi$ in the mass range $0.001 \leq m_\chi \leq 0.1$ GeV. With such statistics, NA64 will also probe other DM scenarios as inelastic DM, and a variety of New Physics extensions such as ALPs, $B - L$ Z' and $L_\mu - L_\tau$ Z', which analysis are currently ongoing. In 2023, we resumed data taking during 56 days accumulating 5.1×10^{11} EOT with an upgraded setup and running at higher intensities, $\sim 6.2 - 6.8 \times 10^6 e^-$/spill.

Furthermore, in this document, we show the first LDM limits obtained using 100 GeV positrons. The analysis performed with 2022 data, 10^{10} positrons on target (e^+OT), demonstrates the positron-missing energy technique. The higher hadron contamination in positron mode is the most critical aspect. This year a dedicated study has obtained the expected contamination level from electron and positron data developing also a complete simulation of the T2 target for both modes [2]. Besides the higher hadron presence, the current level of background is 0.09 ± 0.03. The obtained limits reach the electron ones for a particular Dark Photon mass using a lower statistics. In addition, in 2023, we collected data at lower energy, 70 GeV, to demonstrate that the energy can be scanned and therefore, we will be able to probe different A' mass regions. The NA64 Collaboration plans to submit an addenda for a dedicated positron beam program in the near future.

Besides DM composition, other unresolved low-energy experimental anomalies in Particle Physics such as the long standing muon g-2 anomaly puzzle, have also boosted the interest in DS. The existence of a light Z' gauge boson arising in $L_\mu - L_\tau$ models can accommodate the anomaly and the DM relic explanations. We present the first analysis on $Z' \rightarrow$ invisible searches with 2×10^{10} muons on target (MOT)

collected in the 2022 pilot run at M2. The analysis demonstrates the reliability and control of the missing energy and momentum technique, obtaining a total background of 0.07 ± 0.03. The analysis is still blinded and under collaboration review. The 90% C.L. projected sensitivities obtained in the $(g_{Z'}, m_{Z'})$ plane indicate that we can probe a significant part of the parameter space compatible with the muon g-2 anomaly. In 2023, we have improved significantly the setup, including a second spectrometer to have two independent measurements of the incoming momentum and mitigate the momentum mis-reconstruction level (main source of background). Moreover, we have run at higher intensities collecting 1.5×10^{11} MOT.

In this document, we will describe the three analysis carried out together with a summary of the 2023 runs and our plans for the next year at H4 and M2 beam lines.

2 Summary of the NA64 2022 run at H4 beam line and future prospects

2.1 The $A' \rightarrow$ invisible search: latest results on Light Dark Matter searches

In 2022, we were granted by SPSC 10 weeks of beam time at H4 beam line, from the 27th of July until October 12th. The primary goal for this run was to search for LDM produced through $A' \rightarrow$ invisible decays.

The setup, illustrated in Fig.1, is composed of a set of scintillator and veto counters (S_{0-3} and V_{1-2} in the sketch), a magnet spectrometer consisting of two dipole magnets (MBPL), and a set of tracking detectors which allow tagging the electron incoming beam. The tracking system, four Micromegas chambers (MMs), four straw detectors and two GEM detectors, allows a momentum measurement with a precision of $\delta p/p$ 1% [3]. A synchrotron radiation detector (SRD) [4] is used for electron identification allowing to suppress the hadron contamination in the beam ($\pi/e^- < 3\%$). The active target is a 40 radiation lengths (X0) high-efficiency shashlik electromagnetic calorimeter (ECAL) segmented in a matrix of 5×6 cells made of a sandwich of lead and scintillator plates. The setup is completed with a large high-efficiency VETO counter and three 7.5λ iron hadronic calorimeters (HCALs) to close the hermeticity of the setup measuring any energy leakage. One HCAL module is placed at the zero deflection line to veto charged and neutral secondaries produced from the electron interactions in front of the MBPL magnets. As in 2021, one of the key improvements of the setup is the reduction of the distance between the HCAL and the output window of the vacuum vessel (about 3 m less). This makes the setup more hermetic for detecting hadronic secondaries produced in the upstream e^- interactions with the beam line materials.

The installation, commissioning and calibration of the detectors took 11 days until August 13th. During the first week of data taking we run at lower intensity

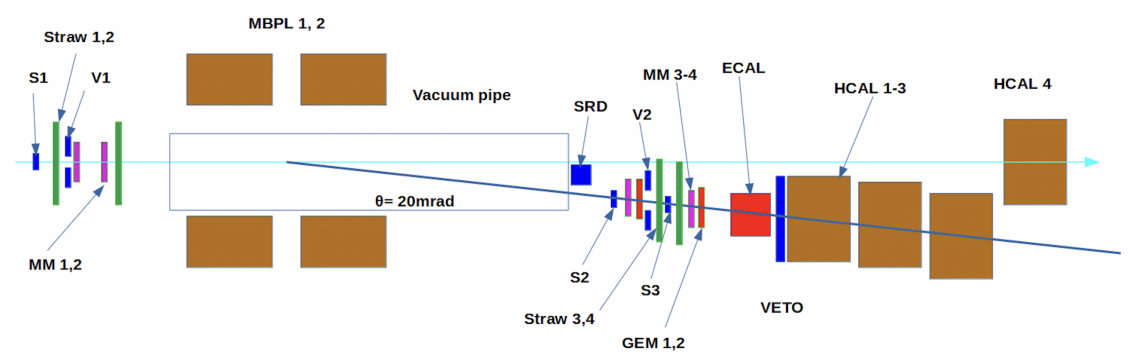

Figure 1. Schematic illustration of the NA64 setup used during 2022 run to search for the $A' \rightarrow$ invisible decay at H4.

$\sim 5.8 \times 10^6$ e$^-$/spill to check the background. In collaboration with the BE-EA department, specially with N. Charitonidis and S. Girod, the beam line was further improved on August 18th adding extra vacuum along the line and removing all beam line elements to reduce material effects. After that, we started data taking at an average intensity of 6.2×10^6 e$^-$/spill, reaching maximum intensities of 6.8×10^6 during the last week of the run. Overall, the units at T2 target were between 80 and 95, having more beam instabilities after the long technical stop in September. We collected during the run a total of 6.26×10^{11} EOT, twice the 2016-2021 total statistics. A summary of the spills recorded during our run is shown in Fig. 2.

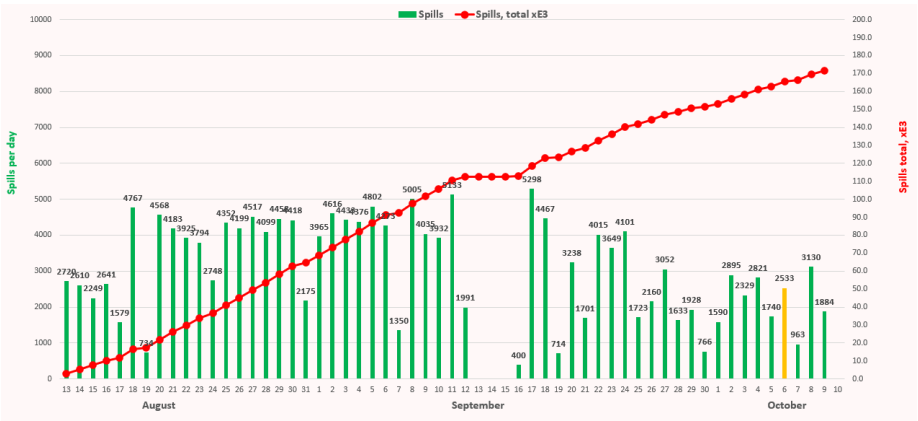

Figure 2. Spills recorded per day during the 2022 run at H4.

The events were recorded with the hardware trigger:

$$Trigger = \Pi S_i \cdot \bar{V}_1 \cdot PS \cdot ECAL \tag{2.1}$$

where PS means that the energy of the pre-shower region of ECAL should be above $\sim$ 0.3 GeV to guarantee that an electron initiated the shower, and $ECAL$ that the energy recorded in the ECAL should be below 90 GeV. The identification of

$A' \rightarrow$ invisible candidates is done by the accurate reconstruction of the initial e^- state and isolating low energy electromagnetic showers in the ECAL, together with no other activity in the VETO and HCAL modules. In Fig.3 the HCAL versus ECAL energy bi-plots is shown after using only the first selection criteria applied, tagging of an initial 100 GeV electron entering the ECAL. Three different regions can be identified in the plot:

- *Region I: These events correspond to the rare QED di-muon production in the target used as a benchmark process to study the accuracy of our MC simulation.*
- *Region II: The diagonal along this region corresponds to the energy conservation line arising from SM events.*
- *Region III: The events visible in this region result from pile-up events.*

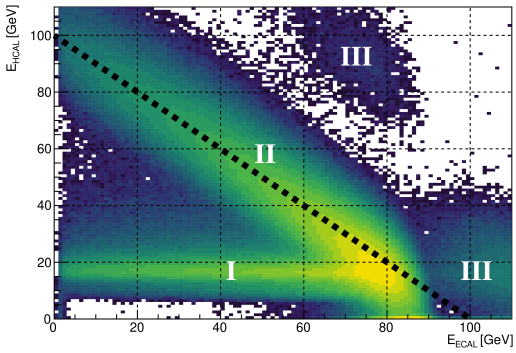

Figure 3. Distribution of events in the E_{ECAL} vs E_{HCAL} plane after applying only beam quality and timing selection to guarantee that an electron has entered into the ECAL. In white letters are illustrated the different types of events (see text for further details).

This year we carried out two independent blind analysis on the 2022 data sample. The signal box was defined as $E_{\mathrm{ECAL}} < 47 - 50$ GeV and $E_{\mathrm{HCAL}} < 1$ GeV depending on the run conditions and detector performance. The minimum energy in the HCAL was determined mostly by the noise of the read-out electronics. The selection criteria applied in the analysis to maximize the acceptance for signal events and to minimize background was similar to the one described in [5] and in previous year report. The main requirements were:

- *Momentum and angle selection of the incoming electron*: only a single track with momenta of 100 ± 10 GeV and an angle with respect to the beam axis within 3 mrad. This cut rejects low energy electrons resulting from upstream interactions leading to large-angle tracks.

- *Particle ID identification*: The energy deposited in each of the three modules of the SRD detector should be compatible with an electron one. This cut is key to reach a 95% electron identification suppressing the hadron contamination in the beam down to a level of $\sim 2 \times 10^{-5}$.

- The lateral and longitudinal shape of the shower should be consistent with an electromagnetic one.

- To reduce background from the upstream hadron electroproduction from e^- interactions before the magnets there should not be multiple hits in the straw detectors (the trackers with higher acceptance) and no signal in the veto and HCALs.

A detailed Monte Carlo simulation using the GEANT4-based DMG4 package [6] was used to study the selection criteria, the signal efficiency, the background level and to estimate the sensitivity. As in the previous analyses, the di-muon sample of events produced in the target was used as a benchmark reaction allowing us to verify the reliability of the MC simulation, correct the signal efficiency vs the A′ energy, cross-check systematic uncertainties and background estimates. The energy distribution for the accepted events after applying all the cuts is depicted in the left panel of Fig. 4.

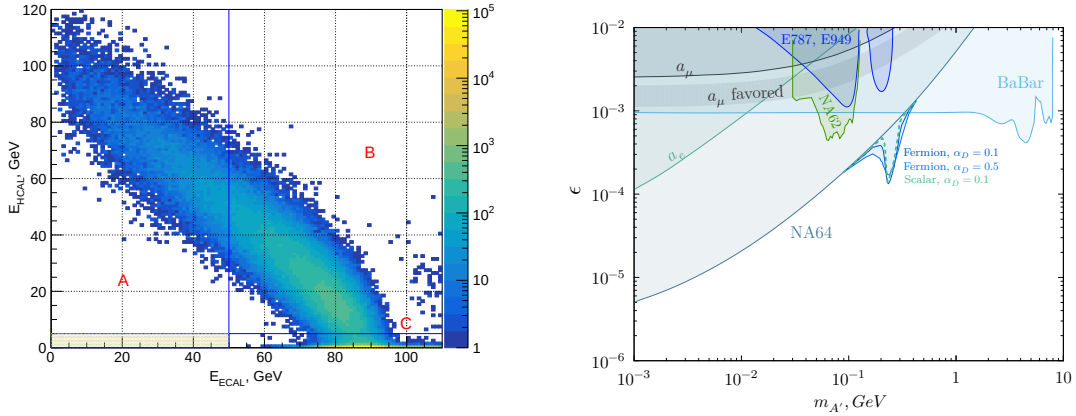

Figure 4. (*Left:)The energy distribution of events in the E_{HCAL} versus E_{ECAL} plane after applying all the selection criteria. (Right:) The 90% C. L. exclusion region in ϵ as a function of the dark photon mass compared to other experiments (further details can be found in [1])*

The background conditions in 2022 run were similar to the 2021 sample. The main background sources affecting the invisible searches for those periods are illustrated in Table 2:

Background source	Background, n_b
1. Di-muons losses or decays in the target	0.04 ± 0.01
2. μ, π, K $\rightarrow$ e +... decays in the beam line	0.3 ± 0.05
3. lost neutrals (γ, n, K^0) from upstream interactions	0.16 ± 0.12
4. Punch-through leading n, K_L^0	< 0.01
Total (conservatively) n_b	0.51 ± 0.13

Table 1. Expected background for the 2021-2022 runs.

The background arising from di-muon losses was estimated from the observed di-muon events and the measured single muon detection efficiency. The second source was evaluated from simulations and measurements from the beam composition (further details about the beam composition will be discussed in the next section). The amount of neutrals escaping the HCAL acceptance resulting from the electro-production of hadrons along the beam line is estimated from data [1, 5]. The background level from these secondaries in the signal box was evaluated by extrapolating the events from the sideband C visible in the left plot of Fig. 4 into the signal region assessing the systematic errors by varying the fit functions. This background source has been reduced in a factor 2 in 2021-2022 runs in comparison with previous years. The last source of background was estimated from the direct measurement of punchthrough events. The final resulting background in the signal region was 0.51 ± 0.13. After unblinding the data, no signal events compatible to $A' \rightarrow$ invisible decay were found in the signal box [1].

This result is used to obtain the combined 90% confidence level (C. L.) upper limits in the mixing strength, ϵ and dark photon mass $m_{A'}$ plane. Those limits are depicted in the right panel of Fig. 4 compared to other experiments. They have been obtained for the 2016-2022 statistics corresponding to 9.37×10^{11} EOT taking into account the different signal efficiencies for all the runs, the background sources and the systematic errors. The main systematic error source is the 10% uncertainty on the signal yield estimate. In addition, the dashed-line region illustrates the enhancement from the inclusion of the resonant annihilation process for different values of α_D.

Combining these results with the thermal freeze-out condition of DM annihilation into the visible sector through the $\gamma - A'$ mixing with strength $e\epsilon$, those limits can be converted into the y= $\epsilon^2 \alpha_D (m_\chi / m'_A)^4$ and m_χ plane. The NA64 limits for two different values of α_D are shown in Fig. 5 compared to the predictions from LDM benchmark models and other experiments (further details and the limits also in the (α_D, m_χ) plane can be seen in [1]). As one can see in the plot, NA64 starts probing for the first time the favoured LDM benchmark models parameter space setting the leading constraints for masses below 350 MeV. DM direct detection experiments such as XENON1T[7], PandaX-4T[8], Damic-M[9], SuperCDMS[10] and DarkSide-50[11] can also set constraints in the LDM parameter space. However, in this case the

sensitivity reach depends on the nature of the DM particle being weaker for the Majorana case [12]. In Fig. 6 the latest results from PandaX-4T[8] are compared to the NA64 and BaBar ones for the scalar case showing the complementarity with accelerator-based techniques. While the coverage from direct detection limits is larger in the high mass region, NA64 leads the searches in the low mass region.

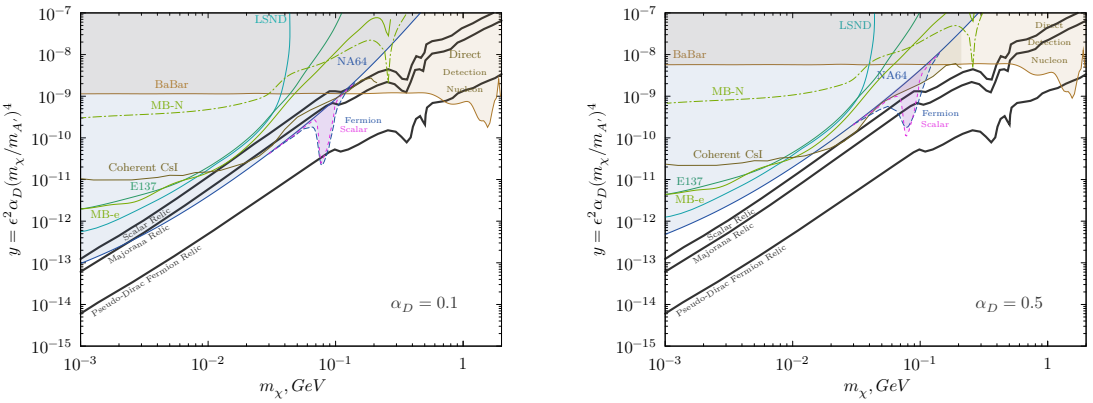

Figure 5. NA64 limits in the (y, m_χ) plane compared to LDM benchmark model predictions for the different DM type (black lines) and to other experiments. We are assuming $m_{A'} = 3m_\chi$ and $\alpha_D = 0.1$ (left plot) and $\alpha_D = 0.5$ (right plot) (see further details in [1]).

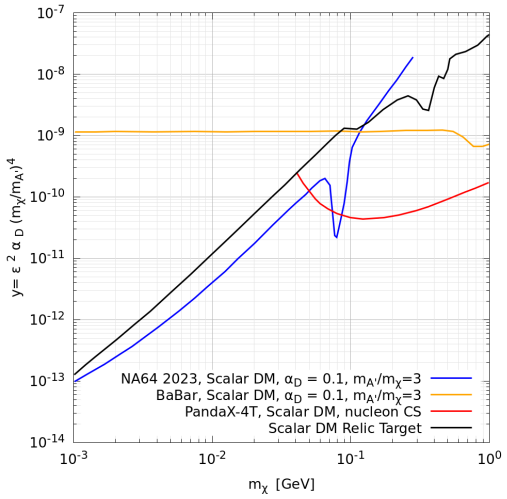

Figure 6. NA64 limits in the (y, m_χ) plane compared to LDM benchmark model predictions for the scalar case compared to BaBar and the latest results from Panda-4T experiment [8].

The exploration of LDM and Dark sectors coupled to electrons has just begun. With the collected statistics, NA64 can also probe a variety of New Physics scenarios involving coupling to electrons. As such, the collaboration is already working on new analysis for light Z' searches in B-L and $L_\mu - L_\tau$ models, inelastic DM and axion-like particles.

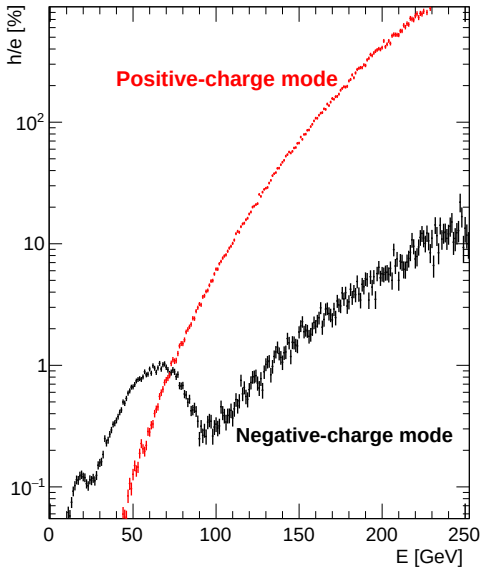

Figure 7. The ratio h/e between hadrons and electrons / positrons at the H4 lead converter, predicted by FLUKA, accounting for the angular and momentum acceptance of the H4 beam line

2.2 Dedicated study of the H4 beam line hadronic contamination

The purity of the electron/positron beam is a critical parameter for the NA64 experiment, since contaminating hadrons are an important source of background events. In particular, the in-flight decay of an impinging hadron upstream the detector to a final state involving a soft electron and an energetic neutrino can mimic the signal signature. The main source of hadron contaminants in the beam is the forward production of long-lived neutral particles in the target, such as Λ hyperons and K_S, propagating downstream and decaying to charged particles after the sweeping magnet.

When the beam line is operated in electron mode, the contamination in the low momentum range, $P \lesssim 100$ GeV/c, is mostly due to the pions from $\Lambda \to p\pi^-$ decay. At larger momentum this contribution drops because of the kinematical limit of the decay process, and the main contribution is due to pions from the K_S decay to a $\pi^+\pi^-$ pair. In positron mode, instead, there is no kinematic suppression at large momentum for the protons from Λ decay. Therefore, a larger intrinsic hadronic contamination of the beam is expected with respect to the electrons one. This effect is illustrated in Fig. 7, showing the H4 beam hadrons-to-electrons (h/e) ratio as a function of the energy in the negative-charge (black) and positive-charge (red) mode, as obtained from a FLUKA-based simulation. A dedicated validation analysis of this prediction was performed, exploiting data collected using only the coincidence of the scintillator counters, finding a very good agreement [2].

2.3 First NA64 results using a 100 GeV positron-beam

A first pilot measurement was also performed during the summer 2022 run using a 100 GeV positron beam impinging the NA64 invisible setup, with a total accumulated statistics of $\simeq 10^{10}$ e^+OT. The main goal of this measurement was to demonstrate, for the first time, the positron-beam missing-energy technique to search for LDM, identifying the corresponding critical items and determining an appropriate strategy to mitigate them, in view of the future NA64 e^+ program. During this measurement, we reversed the H4 beam line optics, obtaining a 100 GeV e^+ beam, and we searched for high missing-energy (> 50 GeV) events compatible with the A' particle production.

The hadronic contamination affecting the positron beam at 100 GeV is higher than that for the electron beam, as discussed in previous section, mostly due to the contribution of protons from the decay $\Lambda \to p\pi^-$ [2]. Consequently, to not overcome the maximum DAQ system acquisition rate, we set the ECAL missing energy trigger threshold to ~ 55 GeV, unavoidably limiting the extension of the sideband region. In addition, we set the trigger energy threshold for the ECAL preshower (ECAL0) at ~ 400 MeV. Due to the kinematic relation between the A' mass and the missing energy induced by the resonance production mechanism, $E_R = M^2_{A'}/(2m_e)$, this choice reflected on the range of accessible $M_{A'}$ values, that was restricted to the $[240, 320]$ MeV interval.

In the analysis, we adopted a blind analysis approach, maximising the signal efficiency for the A' resonant production channel. The adopted selection cuts required the presence of an incoming track with momentum $P \sim 100$ GeV, tagged as a positron by the SRD. Additionally, we selected events in which the shape of the electromagnetic shower in the ECAL was consistent with the expected signal profile for A', and with null activity in the downstream detectors (VETO and HCAL). We estimated the signal yield via a GEANT4-based simulation of the NA64 setup using the DMG4 package [6], applying to Monte Carlo events the same selection cuts used in the data analysis. Moreover, as in the electron case, we exploited the "di-muon" events to optimize the shower-shape cut and validate the MC simulations. Overall, a very good agreement was found.

Due to the high hadronic contamination, the most significant background contribution arises from the upstream decay $K^+ \to e^+\pi^0\nu_e$ of misidentified kaons. If the produced neutrino energy exceeds 50 GeV and the $e^+\gamma\gamma$ particles produce a single low-energy electromagnetic shower in the calorimeter, this decay leads to a dominant background. Similarly, a minor contribution originates from the $\pi^+ \to e^+\nu_e$ decay. The second most significant background channel involves upstream hadron production through the e^+ interaction with the beam line materials [13]. In this case, the low-energy positron impinges on the target while one or more high-energy neutral hadrons are emitted forward at large angles and escape detection. We estimated

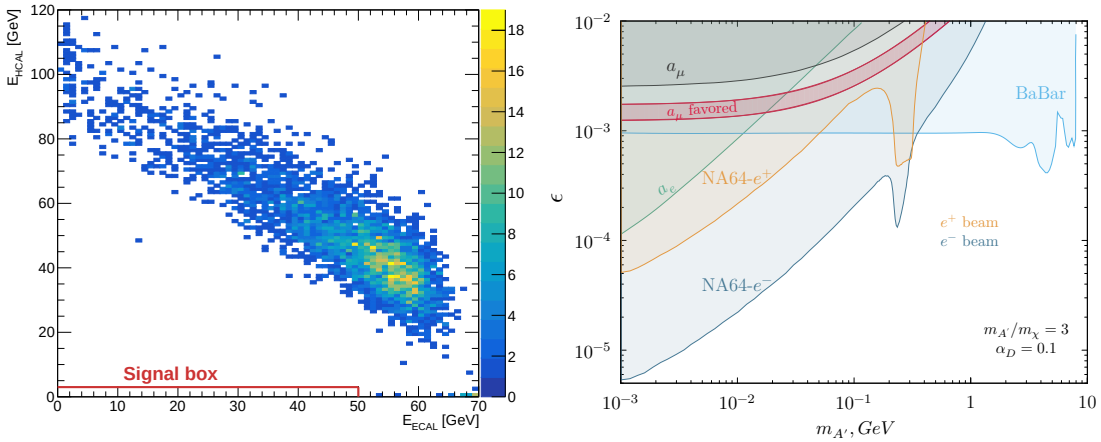

Figure 8. Left: The HCAL vs ECAL energy distribution for events satisfying all analysis cuts. The signal region is also reported (for better visualization, it has been expanded by a factor $\times 3$ along the vertical axis). Right: The obtained sensitivity (orange curve) in the ε vs $m_{A'}$ space for the 100 GeV positron-beam test performed. The most stringent LDM exclusion limits from BaBar [15] and NA64 [1] using 100 GeV electron are also shown, as well as the favored area from the muon $g-2$ anomaly [16, 17] (red lines).

this contribution [14] using the larger dataset collected by NA64 in 2022 with a 100 GeV e^- beam. We performed a dedicated Monte Carlo comparison to ensure that differences between electron and positron hadron production are negligible. Combining all the contributions, a total background yield of $B = (0.09 \pm 0.03)$ events was expected. This result shows the detector's capability to reject hadron-induced background events at 100 GeV e^+ beam energy.

After unblinding the data, no events were observed in the signal region, as reported in Fig. 8. Based on this result, we derived an upper limit on the coupling parameter ε of the A' particle as a function of its mass $m_{A'}$. The obtained exclusion limit is reported in Fig. 8 for fermionic LDM, with $\alpha_D = 0.1$ and $m_{A'} = 3m_\chi$.

In conclusion, we performed the first positron-beam missing-energy measurement searching for LDM, exploiting the existing NA64 setup. In the resonance region, the resulting limits touch our latest electron-beam results corresponding to a $\sim$2 orders of magnitude larger statistics: this proves the feasibility and the potential of a dedicated positron program at NA64. *We foresee to submit a proposal addendum to the SPSC in the near future to start a dedicated experimental program with positrons beam. The goal of this program is to explore the LDM parameter space exploiting the resonant production mechanism at masses where higher sensitivity compared to the electron mode can be achieved.*

2.4 Summary of the 2023 run and future prospects

We resumed data taking on H4 in 2023 on May 10th for 56 days with an upgraded setup, see Fig. 9. The main improvements with respect to 2021-2022 setup are listed below:

- Addition of the new veto hadronic calorimeter (VHCAL) made of Cu-Sc layers. This serves as an additional efficient veto against upstream electroproduction of large-angle hadrons. The detector was tested in 2021 and 2022 NA64$_\mu$ pilot runs at M2, but we did not install it in 2022 to have a large sample of events in 2021 configuration to assess the background level with more statistics. After the analysis of the collected data in 2022 we decided to install it for 2023 run to further reduce the background from neutrals secondaries escaping the HCAL acceptance. We optimised the setup to install the VHCAL without increasing the distance between the HCAL and the end of the vacuum window. In addition, we tried to minimise the amount of material along the line optimising the position of the scintillator counters and trackers after the MBPL magnets. The studies based on Monte Carlo simulations indicated that with such configuration the background will be further reduced. This will be assessed with the collected data sample.

- Placement of a second magnet spectrometer downstream to measure for the first time processes involving muons in the final state after electron interactions in the target. In particular, we will be able to study processes involving $e^- \to \mu$ conversion [18]. The feasibility studies based on simulations to search for such a process were carried out and are summarised here [19]. Moreover, with such improvement we will be able to characterise the energy distribution and the angle between the di-muons produced in the rare QED process. As explained above this is an important benchmark process and thus validating the MC is essential to have reliable estimate of signal efficiency, background and systematics. Such magnet was already placed in 2022 but 15 meters away from the ECAL due to space constraints. In collaboration with the BE-EA department, a way to move closer the magnet was found.

- This year we also included a pre-scaler in our trigger system and recorded events with different type of triggers. In this way, we had always a sub-sample of calibration events, only triggering on scintillator counters and not in ECAL, even during data taking. This allow us to avoid taking additional calibration runs and have a better monitoring of possible energy variations in the calorimeters.

The commissioning and calibration of the detectors, the beam and trigger tuning lasted approximately 10 days. On 21st of May we started collecting data at an intensity between $(6.2 - 6.8) \times 10^6$ e$^-$/spill. This year we had an excellent beam

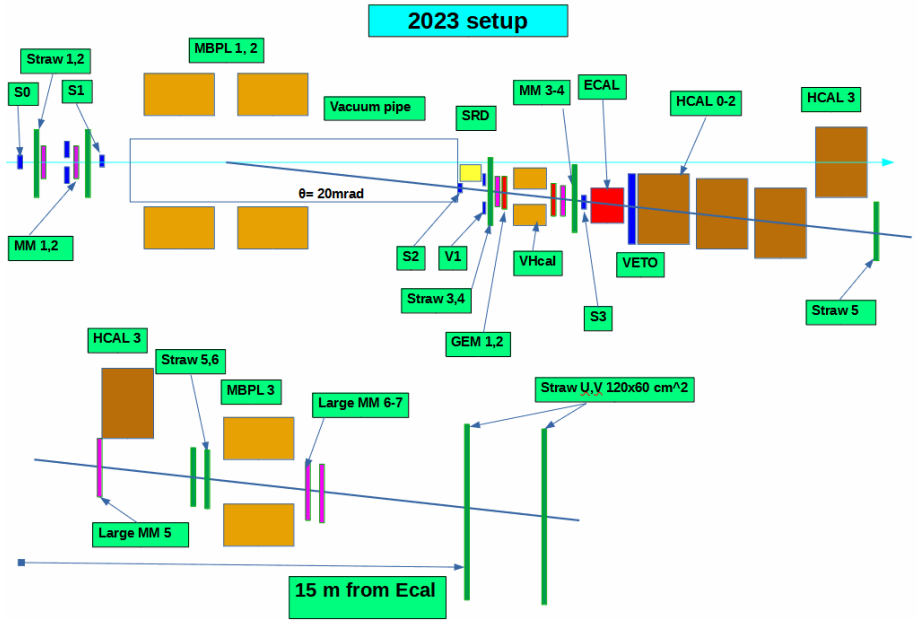

Figure 9. Schematic illustration of the NA64 setup used during 2023 run to search for the $A' \rightarrow$ invisible decay at H4.

quality with most of the time 100 units on average on T2 target and many periods with 3 spill per cycle. In addition, further tuning of the beam and the addition of extra vacuum (performed together with N. Charitonidis and S. Girod) allowed to further reduce the beam halo to 3% and the hadron contamination 0.3% even at higher intensities.

Due to the increase in intensity and in the delivered spills we collected 5.1×10^{11} EOT in 6 weeks. A summary of the spills accumulated along our run is shown in Fig. 10. The last five days of our run are not shown as they were dedicated to: i) perform one day measurements with a positron beam at 70 GeV collecting 1.64×10^{10} positrons on target, and ii) carry out feasibility studies to study the potential of NA64 towards probing DS coupled to quarks collecting $\sim 10^{10}$ hadrons.

The 2016-2023 collected sample corresponds to 1.4×10^{12} EOT. Our goal before the next long-shutdown is to collect 3×10^{12} EOT and continue leading the LDM searches in the low mass region. With such statistics we would be able to probe the LDM parameter space unequivocally for Majorana and scalar DM. For that reason in 2024, we would like to request 10 weeks of beam time at H4 devoted to invisible searches. In addition, as discussed in previous report, in the next two years we plan to complete our detector upgrade using faster digitisers for our MSADC boards to run at higher rates $(1-2) \times 10^7$ e^-/spill after the next shutdown. We plan to be able to test this boards in the foreseen 2025 run before the next shutdown. In the next sub-section we summarise the current status of this development.

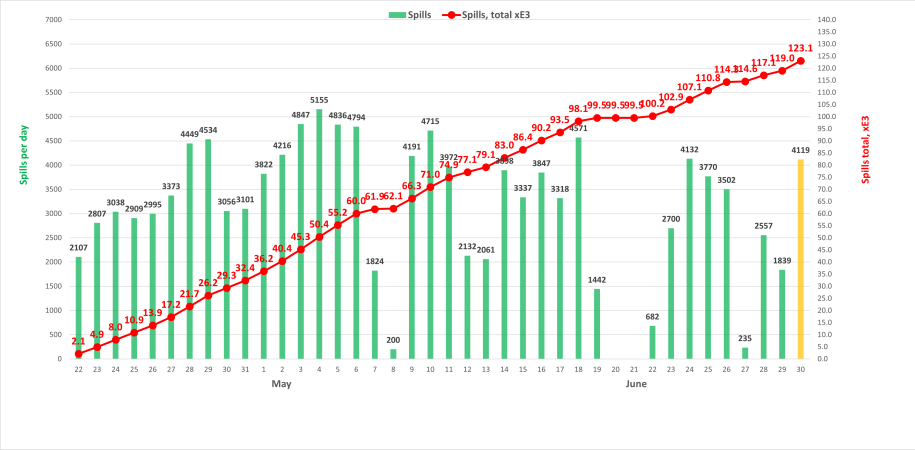

Figure 10. Spills recorded per day during the 2023 run at H4.

2.4.1 Detector upgrades: Status of the new front-end electronics

The possibility to replace the current boards with the "Waveboard" digitizer developed by INFN was already investigated by ad-hoc measurements in 2021 and 2022, demonstrating the improved performances of the system in terms of pile-up reduction and ECAL resolution improvement. These measurements were performed with a standalone firmware, implementing all the features required for NA64 in terms of readout window size, trigger latency, . . ., but still to be integrated in the main NA64 DAQ.

In Autumn 2023, Dr. Fabrizio Ameli and Dr. Stefano Russo, developers of the "Waveboard" device, visited CERN to work together with the NA64 DAQ group toward the integration of the new digitizer in the system. The integration is performed using the custom UCF (Unified Communication Framework) protocol, already used in NA64 to read data from the TDCs reading signals from Straw chambers. First, the data format was modified to be compatible, in terms of control words and channel identifiers, with the one expected from TDCs, in order to avoid any modification to the master DHMux board. Second, a first implementation of the IP cores specific to UCF for the Waveboard was completed, including the hardware-specific ones associated with the GTX fast transceivers connecting the Kintex-7 FPGA with the laser driver. With this firmware version, we were able to start debugging the system, starting from the UCF protocol hand-shaking signals.

We expect to be able to finish the Waveboard integration within the Fall 2023: a dedicated PostDoc, expert in FPGA designing and programming, has been hired from July 2023 at INFN-Genova to work exclusively on this project.

3 Outcome of the 2022 NA64 run at M2 beam line and future plans

3.1 First results using a 160 GeV muon beam

The goal of the NA64μ pilot runs in 2021 and 2022 was to study the feasibility of the missing momentum and energy technique with the 160 GeV muon beam at M2 to search for $Z'(A')$ invisible decays as benchmark processes. More details can be found in our previous year report and in [20, 21]. The outcome of the 2022 spring run was reported in 2022 document, although the analysis of the data was still work in progress. In this report, we summarise the first results using the 160 GeV muon beam demonstrating the feasibility of the missing energy-momentum technique.

The 2022 setup is sketched in Fig. 11. Two beam-defining counters (S_0 and S_1) allow to define a narrow momentum spread of the 160 GeV muon beam impinging on the active target (ECAL). A Z' boson would be produced in the process $\mu Z \to \mu Z Z'$, followed by its prompt invisible decay to neutrinos or DM particles. In this case, the Z'-signature would be a single scattered muon, that has lost more than half of its energy/momentum in the Z' production. For this reason, the inherent feature and challenge of the experiment is to reconstruct accurately the momentum lost by the initial muon and any energy loss in the calorimeters. The tracking system, performs the reconstruction of the muon momentum, upstream of the target with the MS1 spectrometer, and downstream of it, with MS2 (see Fig. 11). MS1 is ~ 80 m long and is composed by a set of bending magnets (BEND6) and several beam-optics defining quadrupoles to focus the beam, together with four Micromegas detectors (MM1-4) and two straw detectors (ST05-4). A set of six Beam Momentum Stations (BMS), BMS1-6, are also placed in the upstream part of the beam line. The challenge of the initial momentum reconstruction is the long lever arm which relies on an accurate definition of the magnetic fields involved and the size of the beam upstream. In addition, the beam is not focused in y and has a momentum spread next to the first BMS station of 4%. One of the improvements of 2022 setup was the addition of $20 \times 20\,\mathrm{cm}^2$ straw stations next to the MMs to have a better knowledge of the beam profile upstream.

The tagged 160 GeV muons collide with the active target, a $40X_0$ shashlik calorimeter composed of a 5×6 matrix made by a sandwich of lead plates and plastic scintillators. After it, a second magnet and a set of GEMs, Micromegas and Straw stations measure the outgoing muon. The scattering of the final state muon (tagged by two counters placed along the beam-deflected axis, S_4 and S_μ) is used to define the trigger to record events at the moderate intensity of $2 \times 10^6 \mu$/spill without efficiency loss (Trigger $= S_0 \times \bar{V_0} \times S_1 \times S_4 \times S_\mu$). In 2022, we took data mostly in two configurations measuring a trigger rate of 0.04-0.07% (with respect to the $S_0 \times \bar{V_0} \times S_1$ rate): i) Trigger 1: $S_4 - 65$ mm and $S_\mu - 152$ mm, and ii) Trigger 2: $S_4 - 65$ mm

and $S_\mu - 117$ mm. The position of the trigger counters determines the detectable momentum range of the scattered muon, in this case a window between 10 and 80 GeV. In addition, the amount of triggered events is dominated by the position of the S_4 counter, as if it is very close to the zero-line one starts triggering on events from the tails of the unscattered beam. As an example, in 2022 we moved it closer increasing the rate up to 0.2%.

To guarantee hermeticity and veto charged and neutral secondaries produced after the muon interaction in the target, the detector is equipped downstream with: a large scintillator VETO (the same used in NA64 at H4), a high-efficiency veto hadronic calorimeter (VHCAL) with an entrance hole of 12×6 cm^2 and two 120×60 cm^2 massive HCALs. A large 120×60 cm^2 straw detector station was built for this run to detect the muon at the end of the setup. Finally, a signal-like event comprises a muon with 160 GeV reconstructed momentum in MS1 and < 80 GeV in MS2, and with total MIP energy in all calorimeters, $E_{\rm CAL} < 12$ GeV.

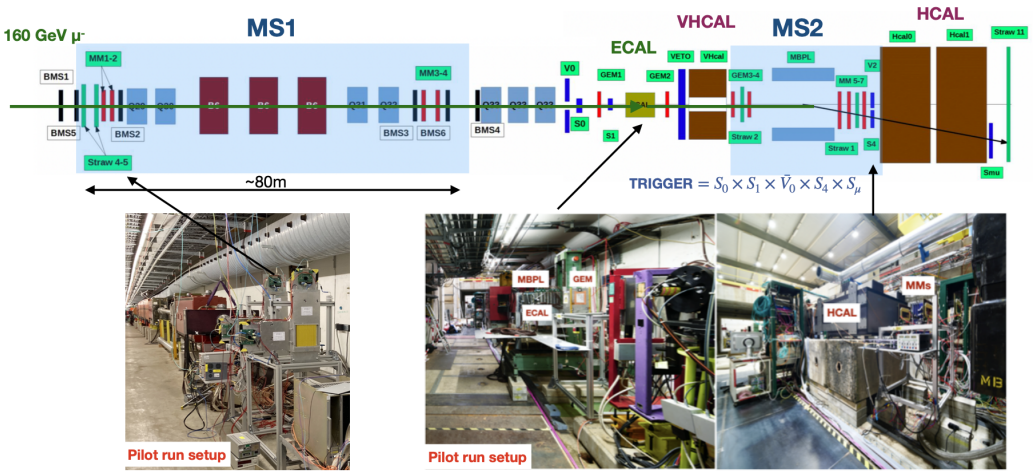

Figure 11. Schematics and pictures of the 2022 NA64$_\mu$ set up at M2 beam-line.

The run was shorter due to an SPS issue, a water leak in the TDC2 near the first splitter magnet. Nevertheless, we accumulated 2×10^{10} MOT with triggers 1 and 2 and a total of 4×10^{10} MOT, taking into account calibration trigger, S_4 placed closer to the beam axis and runs without target (ECAL).

3.1.1 Monte Carlo simulations of the M2 beam line and the signal

A full simulation and reconstruction package using GEANT4 tool-kit [22] and the Geant4 compatible DM package `DMG4` [6] was developed towards having a realistic signal and potential background study. First of all, a realistic M2 beam line optics simulation was developed in collaboration with the CERN BE-EA department, in particular with D. Banerjee and F. Metzger. This includes the definition of all the magnetic elements along the line (quadrupoles QWL and QPL, bending magnets MBN). This framework uses `TRANSPORT`[23], `HALO`[24] and `TURTLE`[25] programs to

transport the particles at the entrance of the set-up, as well as the GEANT4-based beam delivery simulation (BDSIM) program [26–28] to simulate the secondaries interactions along the beam line material. In addition, the differential and total cross-sections for the Dark Z'-Bremsstrahlung process were calculated to have a reliable estimate of the expected signal yield [29]. This year the possibility to simulate scalar and pseudoscalar processes have also been added [30]. Another important step in the simulation, is the implementation of the trigger configuration to account for the Z' acceptance for the different masses. All detectors including the material budget of the different tracking detectors (Micromegas, GEMs, Straws and BMS), as well as all hadronic (VHCAL and HCAL) and electromagnetic (ECAL) calorimeters, trigger counters and vetos have also been included. Finally, the 2022 survey measurements have also been used to accurately place the different detectors (see 12 and 13).

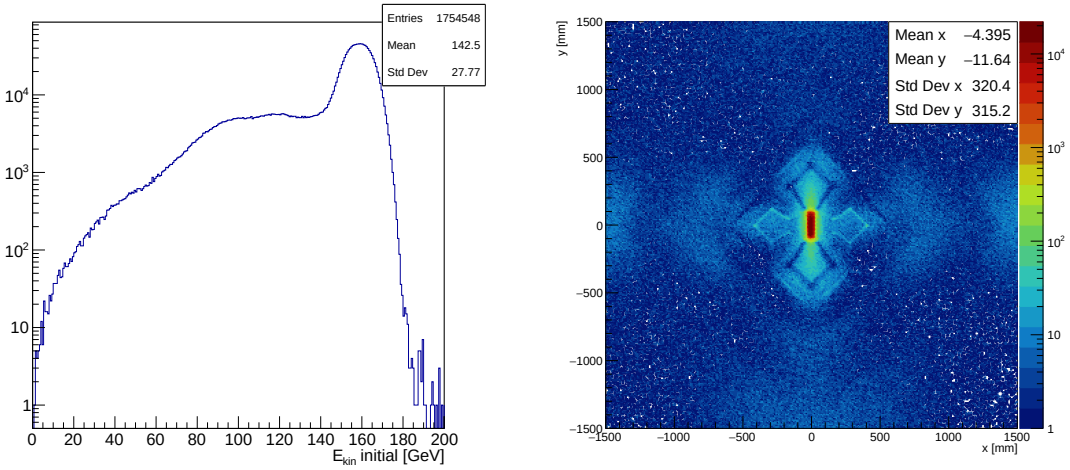

Figure 12. Primary beam muons phase-space as obtained through the BDSIM and MADX programs for their energy spectrum (*Left*) and spatial distribution at the level of BMS1 (*Right*).

3.1.2 Summary of the data analysis

A blinded analysis has been carried out with the signal box defined by the momentum of the outgoing muon below 80 GeV ($p_{\text{out}} < 80$ GeV) and by the sum of all the energies in the calorimeters compatible to the one of a MIP ($\sum \text{CAL} < 12$ GeV). A set of cuts have been defined to maximise the signal over the background using the MC simulation described previously. This simulation has been used to optimise the selection, estimate the sensitivity and study the background level. The cuts are mainly based on two requirements: a MIP traversing the whole setup having a clean signal, namely a single incoming and outgoing reconstructed track. To validate the accuracy of the simulations in reproducing the data, it is necessary to ensure that e.g. simulated energy deposits are well-reproduced, or track-propagation. In Fig. 14

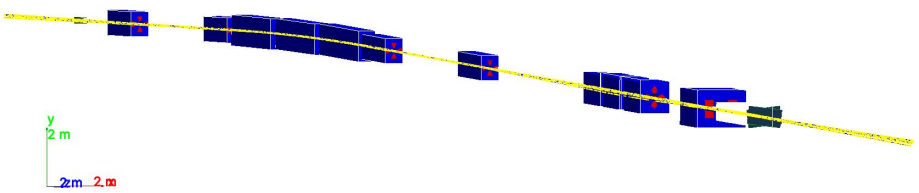

Figure 13. An example of muons propagating along the setup taking into account all the beam line optics elements.

the comparison between energy deposit in the full HCAL (modules 1 and 2) for MC and data (calibration runs) is illustrated. As it is visible in the plot, the MIP peak is well reproduced around ~ 5 GeV.

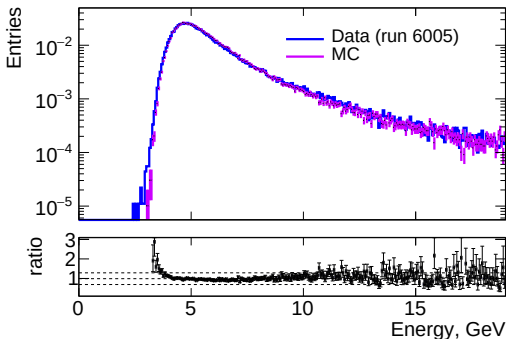

Figure 14. HCAL energy deposit in two modules for (purple) Monte Carlo and (blue) data events from calibration runs. The events are normalized. The MIP peak is well reproduced by the Monte Carlo. Is also shown for completeness the ratio between the two histograms.

The selection criteria that we applied is listed below:

1. *a single muon traversing the set-up*: there is only one single track in the upstream and downstream spectrometers (MS1 and MS2).

2. *initial muon momentum at 160 GeV*: there is one single track selected in the momentum window [140, 180] GeV.

3. *Beam spot*: the beam profile on GEM1 (located before the target) is fitted in both $\hat{x}$ and $\hat{y}$ planes with a Gaussian. It is ensured that the event fits within $\pm 2\sigma$ of the distribution to reduce events from the beam halo.

4. *the initial muon impinges in the ECAL central cell*: the upstream reconstructed track is extrapolated to the ECAL and it is verified that it enters in the ECAL central cell with an energy deposit compatible with the one of a MIP (about ~ 1 GeV).

5. *Single hit in the detectors and clean track after MS2*: the tracking detectors located after the MBPL magnet have at most one hit. The downstream reconstructed track after the bending magnet are extrapolated to the HCAL modules face. The extrapolated position is matched with the given HCAL cell and it is checked whether this is compatible with a MIP (about ~ 2.5 GeV). This procedure is performed over each of the HCAL modules. The tracking detectors after VHCAL should also have maximum one hit to suppress secondaries coming from upstream interactions (e.g. target). This ensures a clean outgoing track within the acceptance of the experimental set-up.

6. *MIP-compatible energy deposit*: in each calorimeter, respectively ECAL, VHCAL and HCAL, the energy deposit is compatible with a MIP (~ 1.0 GeV, ~ 0.7 GeV and ~ 2.5 GeV). Additionally, a MIP signal in the central cell of the Veto is required before VHCAL (~ 6 MeV). An event is accepted if its energy is less than 1.5 of these values. This cut allows to remove events compatible with muon-nuclear interactions in the target.

The events passing the cut-flow selection are shown in the left plot of Fig. 15 in the total energy deposit and outgoing muon momentum plane, $(E_{\mathrm{CAL}}, p_{\mathrm{out}})$. Those events are used to estimate the level of background from non-hermeticity to the signal region. Four main regions are highlighted in the plot: i) region A, associated with MIP compatible events traversing the whole set-up being nearly undeflected; ii) regions B and C respectively associated to events with large energy deposit in the ECAL and the HCAL modules, iii) D composed by events with missing energy resulting from muon-nuclear interactions in the target. Those events result in charged secondaries accompanying the scattered muon. Because of our trigger acceptance, charged particles with energy below 10 GeV will not be inside our experimental acceptance. Thus, these particles can escape the face wall of the first HCAL resulting in non-hermeticity. These processes involving muon-nuclear interactions have been simulated accurately allowing to reproduce the features observed in data.

Out of the previously described regions, we conservatively define two control regions (see Fig. 15, left). The first one (below region D) corresponds to events with large energy deposit on the first HCAL module, being then totally absorbed in the second module. Those events are associated to hadrons produced in upstream interactions before the second magnet spectrometer. The bulk defined in region D is correlated with the trigger configuration, as for the counters S_4 and S_μ being closer to the zero line, muons with higher energy, thus hadrons with lower energy,

are expected to trigger, and vice-versa (see Fig. 15, right). The second region, left of region A is associated with muons traversing the whole set-up and being energy-wise compatible with a MIP. This region allows one to estimate the leakage to the signal region from the tails of the downstream momentum reconstruction. The extrapolated background level from the two control regions using the combined trigger 1 and 2 data is illustrated in Fig. 16

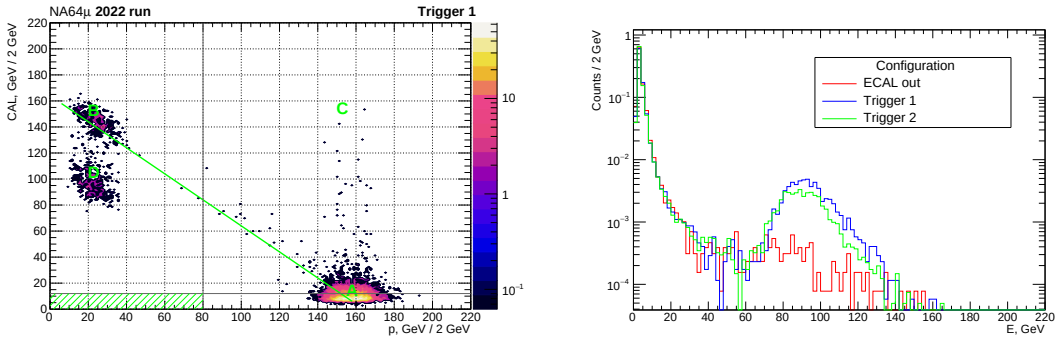

Figure 15. (*Left*) Hermeticity plane (p_{out}, $\sum$CAL) before applying cut on the veto and calorimeters for the trigger 1 configuration runs. The signal box is drawn within the green hased-lined box. Two control regions, below region D and on the left of region A, are defined for the conservative background extrapolation before applying the final set of cuts on the expected MIP signal of the scattered muons. (*Right*) Energy deposit in the first HCAL module after applying the selection cuts up to *Momentum MBP*. The two different trigger configurations are shown, together with the ECAL out runs. The entries are normalized and compatible with region D.

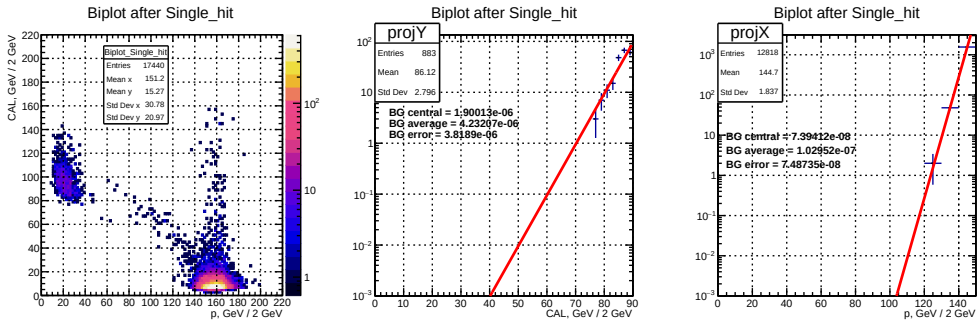

Figure 16. Background extrapolation from the hermeticity plane (*left*) from region D (*middle*) and from region A (*right*) before the MIP-energy selection. The events are selected from the combined trigger configurations 1 and 2.

In addition, two other main sources of background contribute to the estimate of the final background level. The main one is related to momentum mis-reconstruction on MS2. The typical scenario is the correct tagging of the incoming muon with energy $\simeq$ 160 GeV and the mis-reconstruction of its track to $\leq$ 80 GeV whereas it truly

is 160 GeV. This background was estimated using calibration events. A sample of events in the momentum region 160 ± 10 GeV was selected. The background level quoted in the table is obtained after fitting the left tail of the distribution with an exponential and extrapolating it to the low momentum region. Another important source of background is related to the remaining hadron contamination in the M2 beam line being at a level of $P_h \simeq 5 \times 10^{-5}$ per MOT, with $P_{K/\pi} \sim 0.03$ [31]. In particular, kaons can be properly reconstructed with 160 GeV/c momentum in the first spectrometer, BEND6 region, while decaying in flight to muons ($K \rightarrow \mu\nu$) with energy ≤ 80 GeV before the ECAL. A detailed simulation of kaons forcing its decay at the position of the last trackers in MS1 and using the full setup geometry has been performed. The cut-flow selection described in the previous sections has been applied to this sample. The value quoted in the table corresponds to decays resulting in a muon with momentum below 80 GeV passing all our selection criteria with the associated decay products keeping the rest of the energy without suffering interactions in the detectors. Previous work on those backgrounds can also be found in [20] and in [21]. The estimated background levels are summarised in Table 2.

Background source	Background, n_b
Momentum mis-reconstruction	0.045 ± 0.031
Hadron in-flight decays	0.010 ± 0.001
Calorimeter non-hermeticity	< 0.01
Total (conservatively) n_b	0.07 ± 0.03

Table 2. Expected background for the 2022 muon pilot run for 2×10^{10} MOT (trigger 1 and 2 configurations).

The data is still blinded and the analysis note summarising these results is currently under collaboration review. The preliminary 90% C. L. projected sensitivity on the coupling g and mass of the Z' ($m_{Z'}$) has been obtained including the estimated background and considering that the systematic uncertainty on the signal yield amounts (conservatively) to $< 10\%$. The main sources of systematic are listed in table 3 . The high level of purity of the M2 beam line [31], implies that the error on the muons on target is mostly dominated by miscounts in the VME scaler and by possible DAQ crashes. The total error in this case is below 1%. Other source of systematic error comes from the Weiszäcker-William's (WW) approximation used to estimate the production cross-section [32]. The error with respect to ETL is 2% in this case. In addition, other systematics on the ETL cross-section calculation originate from the running of α and soft photon emission (higher order QED corrections) together with the purity of our target. The total systematic due to these uncertainties is about 4%. From the detector point of view, two main sources affect the measurement. The first one is the difference between the calorimeter detector

response in data and in the MC. The systematic error is extracted in each detector from the ratio of the integrated MIP-peak-compatible region estimated in this case to be 4%. The second factor is related to errors from misalignments affecting the scattered muon momentum reconstruction. This number has two contributions. The first one is related to the difference in the particle deflection from MC and data. The second one, is related to the uncertainty on the position of S_4 and S_μ counters. In 2022, these counters were not measured in the survey and the uncertainty in their position was conservatively estimated to be ± 2 mm. We have calculated the difference in the signal yield when the position of the counters is changed by this amount for all the Z' mass range. The error obtained is $< 5\%$ being higher for masses below 100 MeV. In 2023, these counters have been included in the survey measurements and the error in its position is 0.5 mm. This fact will reduce significantly this systematic error in the forthcoming 2023 analysis.

Uncertainty source	Contribution
Number of MOT	0.01
Z' physics	
- WW approx.+Pb purity+Running of α+ Soft photon emission	0.04
Detector response	0.04
Alignment	
- Particle deflection	0.01
- Trigger position	≤ 0.05
Total (conservatively)	≤ 0.08

Table 3. Sources of uncertainty contributing to the systematic on the signal yield.

In Fig. 17 the preliminary results for the Z'-vector and the scalar case are illustrated. As it is visible in the plot, with the 2022 statistics we are able to probe a significant part of the available parameter space suggesting the existence of a new Z' boson as remaining explanation of the muon g-2 anomaly. Besides the Z' process used as benchmark, many other scenarios can also be probed with such statistics. For example, extended $L_\mu - L_\tau$ Z' models, where the new boson can be a portal to LDM. Measurements with the muon beam also allow us to reach a better sensitivity to probe the Dark Photon parameter space in the high mass region (above 100 MeV) in a complementary way to the electron and positron programs. Finally, processes involving Lepton Flavour conversion such as $\mu \to e$ [18, 19, 33] or $\mu \to \tau$ [33, 34] can also be studied.

The results presented in this report demonstrate the proof-of-principle of the missing momentum and energy technique opening the path to the full exploration of DS coupled to muons in the coming years.

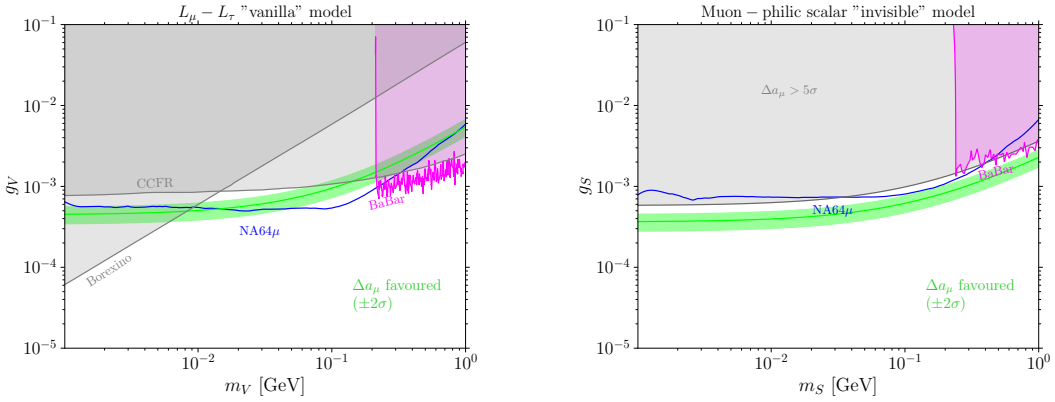

Figure 17. Preliminary NA64μ projected limits (blue) for a (*Left*) light Z' mediator using the statistics corresponding to the trigger configuration 1 and 2 combined. In the figure is also illustrated the $\pm 2\sigma$ band region for the Z' contribution to the $(g-2)_\mu$ discrepancy. For completeness, projected limits for a (*Right*) light scalar S mediator are also shown.

3.2 Summary of the 2023 run and future plans

This year we were granted 28 days of beam time from July 12th until August 9th. The removal of all beam elements in our setup and transport of detectors from H4 beam line started on July, 5th. Thanks to the work carried out by the transport and BE-EA departments most of the equipment was installed on July, 7th. The installation was completed on July 14th, and we started the commissioning and calibration of the detectors. The setup for this run was upgraded following the outcome of the 2022 analysis. The main relevant changes are listed below and a sketch of the setup together with pictures of the main improvements are shown in Fig. 18 and 19:

- The main change introduced this year was the addition of a second magnet spectrometer, MBPL1 in Fig. 18 before our target, as was discussed in our proposal [20]. The addition of this magnet will improve significantly the quality of our data: 1) The initial muon momentum will be measured downstream, closer to our ECAL, where the beam is already focused, avoiding the long level arm and the presence of the beam-optics elements in between. 2) At the same time we will have two independent measurements of the initial muon momentum, one at this spectrometer, and other one at the BMS one. 3) The distance available for the remaining kaons present in the beam to decay in flight will be much shorter reducing also this background source.

- Other important upgrade was the addition of another veto hadron calorimeter in front of our ECAL to further reduce the beam halo.

- To mitigate the momentum mis-reconstruction level this year we had a total of 23 trackers: 11 MMs (eight $8 \times 8cm^2$ and three $25 \times 8cm^2$), 4 GEMs, and

eight straw stations (two $120 \times 60cm^2$ and six $20 \times 20cm^2$).

- The trigger system was also improved, adding an additional scintillator counter, S_2 in the sketch, to have a better muon telescope and select the beam core. In addition, a veto counter, BK, was placed next to S_4 (as foreseen last year) to remove the remaining part of the undeflected beam. The final trigger was $S_0 \times \bar{V_0} \times S_1 \times S2 \times S_4 \times \bar{BK} \times S_\mu$)

- We also included a pre-scaler in our trigger system to record events with two different type of triggers: 1) physical events with the full trigger, $S_0 \times \bar{V_0} \times S_1 \times S2 \times S_4 \times \bar{BK} \times S_\mu$, and 2) calibration events $S_0 \times \bar{V_0} \times S_1 \times S2$.

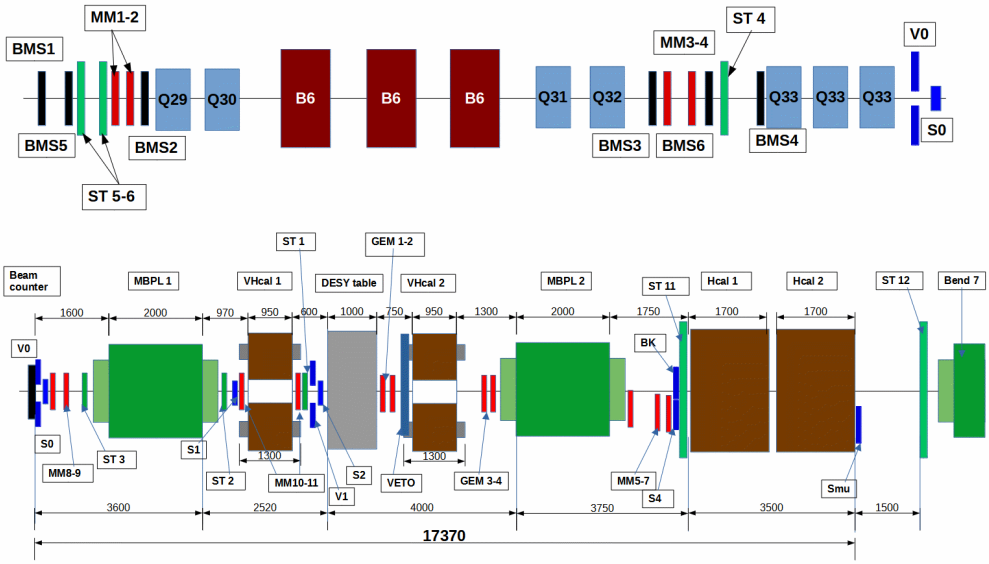

Figure 18. Sketch of the 2023 setup at M2.

It was agreed that until the 20th of July, AMBER will access M2 zone during working hours for the changeover of their setup, coinciding with our commissioning and calibration period. Therefore, we became the main users from July 20th. Overall, the beam quality was excellent during our run, having many periods with 3 spills per cycle with an average intensity on T6 of 35 units. The first three days were devoted to measure the hadron contamination in the M2 beam line. As reported previously, one of the main sources of background arises due to the decay in flight of the remaining kaons in the beam line. In 2022, our run was shorter and we did not have time to measure precisely the level of contamination. This year we carried out this measurement with more granular Berillyum absorbers configuration: 3,4,5,6,7,8

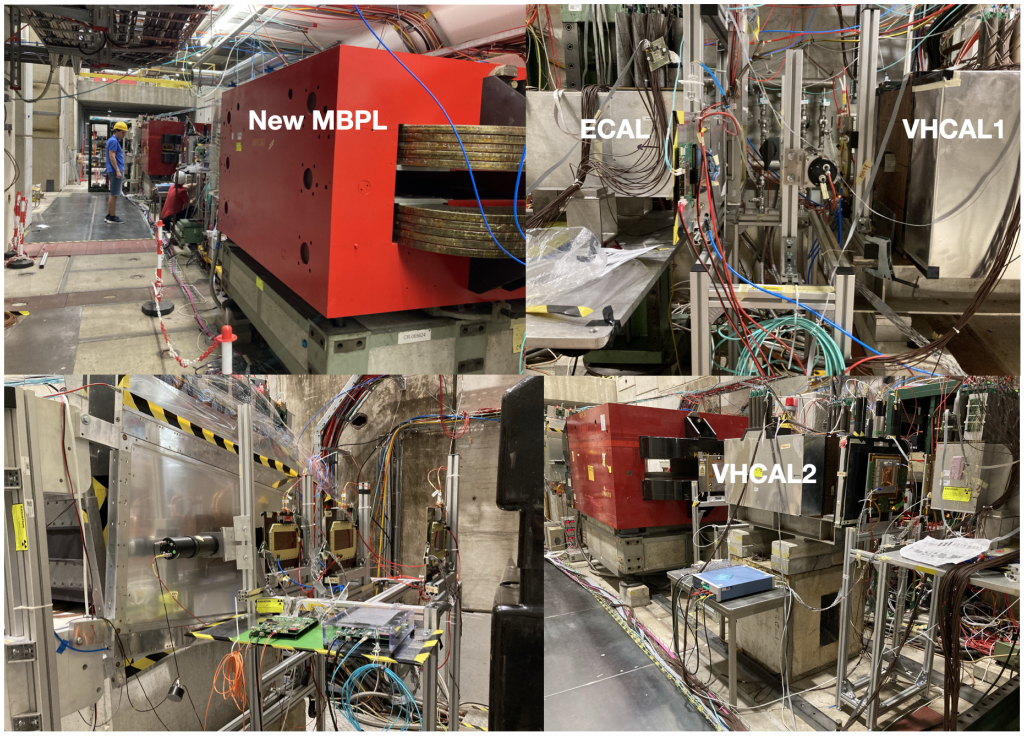

Figure 19. Pictures of the new elements installed for the 2023 run at M2.

and 9. In addition, we are developing new simulations in collaboration with the BE-EA department to compare with the foreseen data results.

On July 23rd, we set up the physical trigger as in 2022 and we reproduce the same trigger rate running at a similar intensity $2.8 \times 10^6 \mu$/spill. We collected 2.2×10^{10} MOT to compare with our previous results. After that, we included the Veto next to S4 in the trigger reducing the rate in a factor 3. On July 25th, we switched on both magnet spectrometers downstream and tune the beam in collaboration with D. Banerjee increasing the intensity up to $4.7 \times 10^6 \mu$/spill. The last day we increase the intensity further running at $10^7 \mu$/spill. In total we collected 1.5×10^{11} MOT, a factor 10 more than in 2022. In addition, we performed the following measurements key to understand the momentum mis-measurements, the main source of background in 2022 analysis: i) we collected 10^{10} MOT without the ECAL, what we refer in previous reports to *empty target measurements*, and ii) we use hadrons at 160 and 80 GeV impinging our setup to study the correlation between the momentum measured in both downstream spectrometers and the HCAL energy.

This year we have demonstrated our working principle. In addition, we were able to run at higher intensity. Thus, our goal before the next long shutdown is to consolidate the exploration of DS weakly coupled to muons collecting $\sim 10^{12}$ MOT. After the next shutdown, we plan to upgrade the experiment to run even at higher intensities to profit the beam capabilities of M2.

We expect to have a preliminary analysis of the 2023 run by the end of the year,

prior to our beam request. If the results are encouraging we plan to request a physics run in 2024.

4 Publications

The collaboration has published the following results since the last report submitted in June 2022:

(i) Y. M. Andreev *et al.* [NA64], "Search for Light Dark Matter with NA64 at CERN," [arXiv:2307.02404 [hep-ex]].

(ii) Y. M. Andreev *et al.* [NA64],"Search for a light Z' in the Lμ-Lτ scenario with the NA64-e experiment at CERN," Phys. Rev. D **106** (2022) no.3, 032015 doi:10.1103/PhysRevD.106.032015 [arXiv:2206.03101 [hep-ex]].

(iii) Y. M. Andreev *et al.* [NA64], "Search for a New B-L Z' Gauge Boson with the NA64 Experiment at CERN," Phys. Rev. Lett. **129** (2022) no.16, 161801 doi:10.1103/PhysRevLett.129.161801 [arXiv:2207.09979 [hep-ex]].

(iv) Y. M. Andreev, *et al.* [NA64] "Measurement of the intrinsic hadronic contamination in the NA64$-e$ high-purity e^+/e^- beam at CERN," [arXiv:2305.19411 [hep-ex]].

In addition, NA64 members and, in particular, the theory working group of the Collaboration, have contributed with the following publications related to NA64e and NA64$_\mu$:

1. V. E. Lyubovitskij, A. S. Zhevlakov, A. Kachanovich and S. Kuleshov, "Dark $SU(2)$ Stueckelberg portal," Phys. Rev. D **107**, no.5, 055006 (2023) doi:10.1103/PhysRevD.107.055006 [arXiv:2210.05555 [hep-ph]]

2. S. N. Gninenko, N. V. Krasnikov, D. V. Kirpichnikov, "Search for Light Dark Matter with accelerator and direct detection experiments: comparison and complementarity of recent results," [arXiv:2307.14865 [hep-ph]].

3. B. Radics, L. Molina-Bueno, L. Fields., H. Sieber and P. Crivelli, "Sensitivity potential to a light flavor-changing scalar boson with DUNE and NA64μ," [arXiv:2306.07405 [hep-ex]] (Accepted in Eur. Phys. J. C on 31st of July).

4. H. Sieber, D. V. Kirpichnikov, I. V. Voronchikhin, P. Crivelli, S. N. Gninenko, M. M. Kirsanov, N. V. Krasnikov, L. Molina-Bueno and S. K. Sekatskii, "Probing hidden sectors with a muon beam: implication of spin-0 dark matter mediators for muon $(g-2)$ anomaly and validity of the Weiszäcker-Williams approach," [arXiv:2305.09015 [hep-ph]] (accepted in Phys. Rev. D the 16th of August).

5. M. Mongillo, A. Abdullahi, B. B. Oberhauser, P. Crivelli, M. Hostert, D. Massaro, L. Molina Bueno and S. Pascoli,"Constraining light thermal inelastic dark matter with NA64," Eur. Phys. J. C **83** (2023) no.5, 391 doi:10.1140/epjc/s10052-023-11536-5 [arXiv:2302.05414 [hep-ph]].

6. I.V. Voronchikhin and D.V. Kirpichnikov, "Resonant probing spin-0 and spin-2 dark matter mediators with fixed target experiments" Phys. Rev. D 107 (2023) 11, 115034

7. Alexey S. Zhevlakov, Dmitry V. Kirpichnikov, and Valery E. Lyubovitskij, "Lepton flavor violating dark photon" arXiv:2307.10771 [hep-ph]

8. I.V. Voronchikhin and D.V. Kirpichnikov, "Probing hidden spin-2 mediator of dark matter with NA64e, LDMX, NA64μ, and M3", Phys. Rev. D 106 (2022) 11, 115041; arXiv: 2210.00751 [hep-ph]

9. A. S. Zhevlakov, D. V. Kirpichnikov and V. E. Lyubovitskij, "Implication of the dark axion portal for the EDM of fermions and dark matter probing with NA64e, NA64μ, LDMX, M3, and BaBar," Phys. Rev. D **106**, no.3, 035018 (2022) doi:10.1103/PhysRevD.106.035018 [arXiv:2204.09978 [hep-ph]].

10. A. Kachanovich, S. Kovalenko, S. Kuleshov, V. E. Lyubovitskij and A. S. Zhevlakov, "Lepton phenomenology of Stueckelberg portal to dark sector," Phys. Rev. D **105**, no.7, 075004 (2022) doi:10.1103/PhysRevD.105.075004 [arXiv:2111.12522 [hep-ph]].

11. Dmitry Gorbunov and Ekaterina Kriukova, "Dark photon production via elastic proton bremsstrahlung with non-zero momentum transfer" arXiv: 2306.15800 [hep-ph]

The collaboration has also contributed to several International Conferences and topical Workshops such as ICHEP2022, IPA2022, LHCP2022, etc where the latest NA64 physics results and the future prospects were presented.

5 Summary

Since our latest report in June 2022, the collaboration has completed several analysis and carried out two new runs in H4 and M2 beam lines. Last year, NA64 performed its longest run at H4 multiplying by three times its 2016-2018 statistics reaching 9.37×10^{11} EOT. In this document, we summarised the pre-print submitted covering the 2016-2022 $A' \to$ invisible searches. We described the analysis detailing the selection criteria applied, the main background sources and the signal sensitivity estimation. The final background in the signal region was 0.51 ± 0.13. After unblinding the data, no signal events compatible with $A' \to$ invisible decay were observed

allowing us to set the most stringent upper limits in the $(\epsilon, m_{A'})$ plane for masses below 350 MeV. Furthermore, the thermal freeze-out condition of DM annihilation into visible matter through the dark photon kinetic mixing with the photon with strength $e\epsilon$, defines a connection between the observed relic DM density and the predicted DM-SM interaction via the dimensionless parameter y= $\epsilon^2\alpha_D(m_\chi/m'_A)^4$. We showed that NA64 limits in the (y, m_χ) plane start probing for the first time the parameter space suggested by the benchmark light Dark Matter models, making further searches extremely exciting and important.

In addition, in 2022 we carried out the first run using 100 GeV positrons collecting $\sim 10^{10}$ positrons on target. The use of positrons enhance the sensitivity via the annihilation channel for a particular dark photon mass. The first LDM searches after a 100 GeV positron beam impinges the NA64 setup have been presented. The main goal of the analysis was to demonstrate the technique, study the potential background sources and identify the critical aspects of the positron mode. As reported last year, the most problematic item is the higher hadron contamination with respect to the electron mode. A detailed study on the hadron contamination ($hadrons/e^{+,-}$ ratio) at H4 in electron and positron modes developing an accurate simulation of the T2 target and the wobbling stations, was carried out by the collaboration. The pre-print is already available in [2]. Due to the higher contamination, the main background source in the positron analysis comes from $K^+ \to e^+\pi^0\nu_e$ decays. In this case, the total background was 0.09 ± 0.03 demonstrating the technique and the reduction of the hadron contamination. The first LDM limits obtained using positrons have also been presented in the document.

In this report, we have also described the first $L_\mu - L_\tau$ $Z' \to$ invisible results from the 2022 pilot run at M2. A total of 2×10^{10} muons on target (MOT) were used for the analysis, which is currently under collaboration review. The obtained level of background was 0.07 ± 0.03, being the main source the momentum misreconstruction. The projected signal sensitivity extracted following the selection criteria and using a realistic Monte Carlo simulation has also been shown. The simulation contains the full experimental setup including all beam-optics elements and the detailed differential and total cross-sections of the $Z'(A')$ Bremsstrahlung process [21, 30, 32]. The reliability of the simulation has been benchmarked also with data. With the collected statistics, NA64 can probe a significant part of the available Z' parameter space compatible with the muon g-2 anomaly. These results demonstrate the robustness of the technique and the potential improvement in the LDM sensitivity for masses above 100 MeV complementing the electron and positron searches. In addition, opens the window to the full exploration of New Physics processes weakly coupled to muons.

Finally, we have summarised the outcome of the spring and summer 2023 runs with upgraded setups at H4 and M2 where 5.1×10^{11} EOT and 1.5×10^{11} MOT were collected. Our plans for the next year have been also depicted, as well as our main

publications since last year.

References

[1] Y. M. Andreev et al. Search for Light Dark Matter with NA64 at CERN (2023).

[2] Y. M. Andreev et al. Measurement of the intrinsic hadronic contamination in the NA64−e high-purity e^+/e^- beam at CERN (2023).

[3] D. Banerjee, P. Crivelli, and A. Rubbia. *Adv. High Energy Phys.* 2015, 105730 (2015). doi:10.1155/2015/105730.

[4] E. Depero et al. *Nucl. Instrum. Meth. A* 866, 196 (2017). doi:10.1016/j.nima.2017.05.028.

[5] D. Banerjee et al. *Phys. Rev. Lett.* 123, 121801 (2019). doi:10.1103/PhysRevLett.123.121801.

[6] M. Bondi, et al. *Comput. Phys. Commun.* 269, 108129 (2021). doi:10.1016/j.cpc.2021.108129.

[7] E. Aprile et al. *Phys. Rev. Lett.* 123, 251801 (2019). doi:10.1103/PhysRevLett.123.251801.

[8] D. Huang et al. (2023).

[9] I. Arnquist et al. *Phys. Rev. Lett.* 130, 171003 (2023). doi:10.1103/PhysRevLett.130.171003.

[10] M. F. Albakry et al. *Phys. Rev. D* 107, 112013 (2023). doi:10.1103/PhysRevD.107.112013.

[11] P. Agnes et al. *Eur. Phys. J. C* 83, 322 (2023). doi:10.1140/epjc/s10052-023-11410-4.

[12] S. N. Gninenko, et al. (2023).

[13] S. N. Gninenko, et al. *Phys. Rev. D* 94, 095025 (2016). doi:10.1103/PhysRevD.94.095025.

[14] D. Banerjee et al. *Phys. Rev. D* 97, 072002 (2018). doi:10.1103/PhysRevD.97.072002.

[15] J. P. Lees et al. *Phys. Rev. Lett.* 119, 131804 (2017). doi:10.1103/PhysRevLett.119.131804.

[16] M. Pospelov. *Phys. Rev. D* 80, 095002 (2009). doi:10.1103/PhysRevD.80.095002.

[17] B. Abi et al. *Phys. Rev. Lett.* 126, 141801 (2021). doi:10.1103/PhysRevLett.126.141801.

[18] S. N. Gninenko and N. V. Krasnikov. *Phys. Rev. D* 106, 015003 (2022). doi:10.1103/PhysRevD.106.015003.

[19] A. Ponten. Sensitivity study of a dark leptonic scalar portal at na64. https://doi.org/10.3929/ethz-b-000584300 (2022).

[20] D. Banerjee *et al.* [NA64 Collaboration]. Proposal for an experiment to search for dark sector particles weakly coupled to muon at the CERN SPS, CERN-SPSC 2019-002/ SPSC-P-359 (2019).

[21] H. Sieber, et al. *Phys. Rev. D* 105, 052006 (2022). doi:10.1103/PhysRevD.105.052006.

[22] S. Agostinelli et al. *Nucl. Instrum. Meth. A* 506, 250 (2003). doi:10.1016/S0168-9002(03)01368-8.

[23] K. L. Brown, et al. (1983). doi:10.5170/CERN-1980-004.

[24] C. Iselin (1974). doi:10.5170/CERN-1974-017.

[25] K. L. Brown and F. C. Iselin (1974). doi:10.5170/CERN-1974-002.

[26] L. J. Nevay et al. *Comput. Phys. Commun.* 252, 107200 (2020). doi:10.1016/j.cpc.2020.107200.

[27] L. J. Nevay, et al. *CERN Yellow Rep. Conf. Proc.* 2, 45 (2020). doi:10.23732/CYRCP-2018-002.45.

[28] L. Nevay, et al. In *10th International Particle Accelerator Conference*, page WEPTS058 (2019). doi:10.18429/JACoW-IPAC2019-WEPTS058.

[29] D. V. Kirpichnikov, V. E. Lyubovitskij, and A. S. Zhevlakov. *Phys. Rev. D* 102, 095024 (2020). doi:10.1103/PhysRevD.102.095024.

[30] H. Sieber, et al. (2023).

[31] N. Doble, et al. *Nucl. Instrum. Meth. A* 343, 351 (1994). doi:10.1016/0168-9002(94)90212-7.

[32] D. V. Kirpichnikov, et al. *Phys. Rev. D* 104, 076012 (2021). doi:10.1103/PhysRevD.104.076012.

[33] S. Gninenko, et al. *Phys. Rev. D* 98, 015007 (2018). doi:10.1103/PhysRevD.98.015007.

[34] B. Radics, et al. Sensitivity potential to a light flavor-changing scalar boson with DUNE and NA64μ (2023).